A unique capsular polysaccharide structure from the psychrophilic marine bacterium *Colwellia psychrerythraea* 34H that mimicks antifreeze (glyco) proteins

Sara Carillo,[#^] Angela Casillo,[#^] Giuseppina Pieretti,[#] Ermenegilda Parrilli,[#] Filomena Sannino,[#,§] Maddalena Bayer-Giraldi,[†] Sandro Cosconati,[◊] Ettore Novellino, [⊥]Marcela Ewert,[‡] Jody W. Deming,[‡] Rosa Lanzetta,[#] Gennaro Marino,[#] Michelangelo Parrilli,[#] Antonio Randazzo,[⊥] Maria L. Tutino,[#*] M. Michela Corsaro[#*]

[#]Department of Chemical Sciences, University of Naples "Federico II", Complesso Universitario Monte S. Angelo, Via Cintia 4, 80126 Naples, Italy

[§]Institute of Protein Biochemistry, CNR, Via Pietro Castellino 111, 80131 Naples, Italy

[‡]School of Oceanography, University of Washington, Box 357940, 98195, Seattle, WA, USA

[†]Alfred-Wegener-Institut Helmholtz-Zentrum für Polar- und Meeresforschung (AWI), Am Alten Hafen 26, 27568 Bremerhaven, Germany

[⊥]Department of Pharmacy, University of Naples "Federico II", Via D. Montesano, 49, 80131 Naples, Italy

[◊]DiSTABiF, Seconda Università di Napoli, Via Vivaldi 43, 81100 Caserta, Italy

Supporting Information

ABSTRACT: The low temperatures of polar regions and high altitude environments, especially icy habitats, present challenges for many microorganisms. Their ability to live under subfreezing conditions implies the production of compounds conferring cryotolerance. *Colwellia psychrerythraea* 34H, a γ-proteobacterium isolated from subzero Arctic marine sediments, provides a model for the study of life in cold environments.

We report here the identification and detailed molecular primary and secondary structures of capsular polysaccharide from *C. psychrerythraea* 34H cells. The polymer was isolated in the water layer when cells were extracted by phenol/water and characterized by one- and two-dimensional NMR spectroscopy together with chemical analysis. Molecular mechanic and dynamic calculations were also performed. The polysaccharide consists of a tetrasaccharidic repeating unit containing two amino sugars and two uronic acids bearing threonine as substituent. The structural features of this unique polysaccharide resemble those present in antifreeze proteins and glycoproteins. These results suggest a possible correlation between the capsule structure and the ability of *C. psychrerythraea* to colonize subfreezing marine environments.

Introduction

Cold-adapted bacteria are microorganisms able to thrive in habitats where the average temperatures are permanently or transiently below 15 °C, and often well below that value. They have successfully colonized all cold environments, including alpine and polar settings, the deep ocean, caves, terrestrial and ocean subsurface, and the upper atmosphere. Besides a general interest in understanding mechanisms underlying their ability to survive and grow at temperatures near or below the freezing point of water, in recent years cold-adapted microorganisms have received extra consideration due to the potential biotechnological applications of their enzymes.[1-3]

Because microorganisms are at thermal equilibrium with their environment, it is reasonable to assume that structural and functional components in psychrophiles (optimal growth at ≤ 15°C) have adapted, to some degree, to the requirements of a low temperature existence,[4] including the possible presence of ice crystals in their immediate surroundings.

The reported mechanisms of bacterial adaptation to low temperature include the over-expression of cold-shock and heat-shock proteins, the presence of unsaturated and branched fatty acids that maintain membrane fluidity,[5] the different phosphorylation of membrane proteins and lipopolysaccharides,[6-11] and the production of cold-active enzymes,[12] antifreeze proteins and cryoprotectants.[13] The latter are chemical substances that generally include small molecules, such as glycine betaine, some amino acids, sugars (glucose, fructose) and sugar alcohols (mannitol, glycerol). However, in the last decade, the high molecular mass extracellular exudates of psychrophiles have reached a prominent position among the cryoprotectants.[14,15] These exudates, which are a rich source of carbohydrate-containing compounds, influence the physico-chemical environment of bacterial cells and are believed to contribute to numerous processes involved in microbial cold-adaptation.

The potential roles of extracellular polysaccharide substances (EPS) in the cold-adapted bacterial lifestyle have been investigated from both the environmental and organismal perspectives.[16-18] Initial chemical characterizations of EPS produced and secreted by cold-adapted bacteria in culture have revealed complex mixtures composed primarily of large sugar compounds, with lesser fractions of protein, lipid, and various small molecules. Nichols and coauthors demonstrated that exopolysaccharides produced by Antarctic bacteria were very diverse and that most of the EPS contained charged uronic acid residues; several also contained sulfate groups and some strains produced large polymers.[19] The presence of EPS can also alter interactions between the cell and the environment because EPS coatings determine the surface chemistry reactivity of cells by increasing the type and number of

functional groups available for interaction, as demonstrated for the cold-adapted organism *Hymenobacter aerophilus*.[20]

Despite their important roles in cryoprotection and environmental interactions, few exopolysaccharide structures from cold-adapted bacteria have been accurately elucidated.[7,19,21] In addition, an increased understanding of the structural characteristics of these polymers is a prerequisite to potential biotechnological exploitation of cold-adapted bacterial EPS.

Colwellia psychrerythraea 34H is a Gram-negative bacterium belonging to the phylum γ-proteobacteria. Enriched from Arctic marine sediments at –1 °C, it proved to be strictly psychrophilic.[18] *C. psychrerythraea* 34H produces extracellular polysaccharides[12,22] with cryoprotectant function and apparent ice-affinity,[23,24] yet its structural characteristics are not well known. In this study, we demonstrated that under the applied growth conditions *C. psychrerythraea* 34H cells are characterized by the presence of a capsule, which was purified as capsular polysaccharide (CPS) and subjected to complete structural determination. We further investigated the three dimensional structure of the macromolecule by molecular mechanic and dynamic calculations. The results revealed an intriguing model, where the apparent "zigzag" structure exhibits on the edge putative ice-interaction sites.

Materials and Methods

Cell growth. *Colwellia psychrerythraea* 34H[12,22] was grown aerobically at 4 °C in Marine Broth medium (DIFCO™ 2216). When the liquid culture reached late exponential phase (OD_{600} = 2), cells were harvested by centrifugation for 20 min at 5000 rpm and 4 °C. Cells used for transmission electron microscopy were grown at 4 °C as colonies on a 15% agar-containing Marine Broth plate.

Transmission electron microscopy (TEM). TEM analysis was performed by the Interdepartmental Centre for Electron Microscopy Service, University of Naples Federico II. The samples were prepared for TEM observations as detailed in Basile et al.[25] Briefly, specimens were fixed with 3% glutaraldehyde, post-fixed with 1% osmium tetroxide, dehydrated with ethanol up to propylene oxide and embedded in Spurr's epoxy medium. Ultrathin sections (60 nm thick) were collected on copper grids and stained with uranyl acetate and lead citrate. A FEI EM 208S transmission electron microscope, with an accelerating voltage of 80 kV, was used for observations.

CPS isolation and purification. Dried cells (4.8 g) were extracted first with phenol/chloroform/light petroleum (PCP) method to recover lipooligosaccharide (LOS) for core oligosaccharide structural characterization[26] and then by hot phenol/water method as reported previously.[27,28] A 300 mg amount of water extract was dialyzed and then digested with proteases, DNAses and RNAses to remove contaminating proteins and nucleic acids. The water extract was hydrolyzed with 1% aqueous CH_3COOH (9 mL, 100 °C, 5 h). The resulting suspension was then centrifuged (10,000g, 4 °C, 30 min). The pellet was washed twice with water and the supernatant layers were combined and lyophilized (80 mg). The supernatant portion was then fractionated on a Biogel P-10 column (Biorad, 1.5 x 130 cm, flow rate 17 mL/h, fraction volume 2.5 mL), eluted with water buffered (pH 5.0) with 0.05 M pyridine, and 0.05 M acetic acid, obtaining two fractions. The first, eluted with the void volume, contained a polysaccharidic material (25 mg), while the second was constituted by oligosaccharides (48 mg). The polysaccharidic material was further purified on a Sephacryl S-400HR (Sigma, 1 x 110 cm, flow rate 15.6 mL/h, fraction volume 2.5 mL) eluted with 0.05 M ammonium hydrogen carbonate, providing a major fraction containing a fairly pure polysaccharide (CPS, 6 mg). Details of chromatography can be found in SI.

DOC-PAGE analysis. PAGE was performed using the system of Laemmli[29] with sodium deoxycholate (DOC) as detergent. The separating gel contained final concentrations of 14% acrylamide, 0.1% DOC and 375 mM Tris/HCl (pH 8.8); the stacking gel contained 4% acrylamide, 0.1% DOC and 125 mM Tris/HCl (pH 6.8). LPS samples were prepared at a concentration of 0.05 % in the sample buffer (2% DOC and 60 mM Tris/HCl [pH 6.8], 25% glycerol, 14.4 mM 2-mercaptoethanol, and 0.1% bromophenol blue). All concentrations are expressed as mass/vol percentage. The electrode buffer was composed of SDS (1 g/L), glycine (14.4 g/L) and Tris (3.0 g/L). Electrophoresis was performed at a constant amperage of 30 mA. Gels were fixed in an aqueous solution of 40% ethanol and 5% acetic acid. Lipooligosaccharide (LOS) bands were visualized by both silver staining and Alcian blue as described previously.[30,31]

Static Light Scattering (SLS). SLS measurements were performed as reported.[32] A home-made instrument composed by a Photocor compact goniometer, a SMD 6000 Laser Quantum 50 mW light source operating at 5325 Å, a photomultiplier (PMT-120-OP/B) and a correlator (Flex02-01D) from Correlator.com was used. All measurements were performed at (25.00 ± 0.05) °C with temperature controlled through the use of a thermostat bath. The mass-average molecular weight, Mw, was obtained from the equation: $K_{LS}C_1/R_\theta = 1/M_w + 2BC_1$ at two different concentrations of C_1 (1mg/mL and 0.5 mg/mL), where C_1 is the CPS mass concentration, B is the second virial concentration, and $K_{LS} = 4\pi^2 n_0^2 (dn/dc_1)^2 / N_A \lambda^4$, where n_o = 1.33 is the refractive index of water, (dn/dc_1) is the refractive index of CPS, and λ is the laser wavelength. The excess Rayleigh ration was measured at two different angles (θ = 90° and 40°). The values of R_θ were calculated by using toluene as reference. From the extrapolation of the scattering intensity of the two solutions at 0 concentration and the 0 angle (Zimm plot) the molecular weight was evaluated.

Sugar and amino acid analysis. Monosaccharides were analyzed as acetylated methyl glycosides. Methanolysis was performed in 1.25 M HCl/MeOH (0.5 mL, 80 °C, 20 h) and the sample was extracted twice with hexane. The organic layer containing the fatty acids methyl esters was directly analyzed, while the methanol layer was dried and acetylated with Ac_2O and pyridine (50 μL, 100 °C, 30 min). Methylation was performed with CH_3I in DMSO and NaOH (20 h).[33,34] The product was carboxymethyl reduced with $NaBD_4$, hydrolyzed with 2 M TFA (120 °C, 2 h), reduced with $NaBD_4$, and finally acetylated with Ac_2O and pyridine (50μL each, 100 °C, 30 min). The absolute configuration of the sugars was determined by gas-chromatography analysis of their acetylated *(S)*-2-octyl glycosides, while the absolute configuration of the amino acid residue was inferred by analyzing its butyl ester derivative.[35] All the samples were analyzed on an Agilent Technologies gas chromatograph 6850A equipped with a mass selective detector 5973N and a Zebron ZB-5 capillary column (Phenomenex, 30m x 0.25mm i.d., flow rate 1 mL/min, He as carrier gas). Acetylated methyl glycosides were analyzed accordingly with the following temperature program: 150 °C for 3 min, 150 °C→240 °C at 3°C/min. For partially methylated alditol acetates the temperature program was: 90 °C for 1 min, 90 °C→140 °C at 25 °C/min, 140 °C→200 °C at 5 °C/min, 200 °C→280 °C at 10 °C/min, and 280 °C for 10 min. Analysis of acetylated octyl glycosides was performed at 150 °C for 5 min, then 150 °C→240 °C at 6 °C/min, and 240 °C for 5 min, while analysis of acetylated butyl ester of the amino acid was performed at 100° C for 2 min, 100 °C→180 °C at 3 °C/min, then 180 °C→300 °C at 15 °C/min.

NMR spectroscopy. ^{1}H and ^{13}C NMR spectra were recorded using a Bruker Avance 600 MHz spectrometer equipped with a cryo-probe. All two-dimensional homo- and heteronuclear experiments (double quantum-filtered correlation spectroscopy, DQF-COSY; total correlation spectroscopy TOCSY; rotating-frame nuclear Overhauser enhancement spectroscopy, ROESY; Nuclear Overhauser Effect Spectroscopy, NOESY; distortionless enhancement by polarization transfer-heteronuclear single quantum coherence, ^{1}H-^{13}C DEPT-HSQC; heteronuclear multiple bond correlation, ^{1}H-^{13}C HMBC; and 2D *F2*-coupled HSQC) were performed using standard pulse sequences available in the Bruker software. The mixing time for TOCSY and ROESY experiments was 100 ms. NOESY experiments were performed at mixing times of 70, 100, 150 and 200 ms, in order to identify genuine NOEs effects. Chemical shifts were measured at 298 K in D_2O. TOCSY (mixing time 100 ms) and NOESY (mixing time 200 ms) experiments were also performed in H_2O/D_2O 9:1.

Structure Calculations. A simplified model of the polysaccharide having about five repetitions of the tetra-saccharide A-B-C-D **(M1,** Figure 5a**)** was constructed through the carbohydrate builder within the Glycam web server[36] while the Thr residue attached to the α-galactopyranuronic acid was constructed employing the builder module in the Maestro package of the Schroedinger Suite 2014. Restrained Simulated Annealing (SA) calculations were performed on M1 using the AMBER 14.0 package[37] with sugars described by the latest GLYCAM06 force field (GLYCAM_06j-1);[38] parameters for Thr residue were retrieved from the ff14sb force field within the AMBER 14.0 package as well as missing bond parameters. For annealing simulations, the General Born solvation (igb = 2) with monovalent salt concentration corresponding to 0.1 M was used. The complex was heated to 600 K in the first 5 ps, cooled to 100 K for the next 13 ps, and then cooled to 0 K for the last 2 ps. The temperature of the system was maintained with a varying time constant: 0.4 ps during heating, 4 ps during cooling to 100 K, 1 ps for the final cooling stage, and then reduced from 0.1−0.05 for the last picosecond. The force constants for NOE constraints were increased from 3 to 30 kcal mol^{-1} $Å^{-2}$ during the first 5 ps and then maintained constant for the rest of the simulation. These force constants were applied in the form of a parabolic, flat-well energy term where *r* is the model distance or torsion angle and *k* is the respective force constant.

$$E_{constraint} = k(r_2 - r)^2 \qquad r_1 \le r < r_2$$

$$E_{constraint} = 0 \qquad r_2 \le r \le r_3$$

$$E_{constraint} = k(r_3 - r)^2 \qquad r_3 \le r < r_4$$

The values for r_1 and r_4 represent upper and lower distance bounds, defining the energetic penalty before and after the flat-well energy term. The upper distance bounds were retrieved by NOE cross-peak volume integrations performed with the iNMR (www.inmr.net), using the NOESY experiment collected at mixing time of 100 ms. The NOE volumes were then converted to distance restraints after they were calibrated using the known fixed distance ($H6_aD/H6_bD$) (Tables S1 and S2).

An unrestrained energy minimization step completed the simulated annealing run. This simulated annealing/energy minimization procedure was repeated 200 times. SA simulations were then analyzed by clustering the resulting **M1** conformations through the average linkage method and a cluster member cutoff of 1.25 Å rmsd calculated on the sugars rings atoms within the central 2 repetitions of the tetramer A-B-C-D. This clustering allowed selecting 33 different conformational clusters for which the most populate one had a frequency of occurrence of 51/200 conformations. Moreover, conformations of this latter cluster feature the lowest overall potential energy and NMR restraint violations. Thus, the representative structure (i.e. the closest to the centroid of the cluster) of this cluster was considered for subsequent molecular dynamics simulations. After charge neutralization by the addition of 11 Na^+ ions, the complex was solvated with 10277 water molecules in a truncated octahedral box of pre-equilibrated TIP3P water.[39] Several equilibration steps were performed comprising minimization of the solvent molecules with the polysaccharide **M1** fixed, minimization of the whole system, and slow heating to 300 K with weak positional restraints on **M1** atoms under constant-volume conditions. The following 20 ns production runs were applied in the NPT ensemble. The particle mesh Ewald method[40] was used to evaluate the electrostatic interactions with a direct space sum cutoff of 10 Å. With the bond lengths involving hydrogen atoms kept fixed with the SHAKE algorithm, a time step of 2 fs was employed.[41] Related conformational substates populated during the molecular dynamics simulation were analyzed with the AMBERS's PTRAJ module.[42] For the production run trajectory, the first frame configuration was taken as a reference for subsequent mass-weighted rmsd calculations considering all atoms excluding hydrogens. Illustrations of the structures were generated using Chimera.[43]

Ice recrystallization inhibition assay. Ice recrystallization was measured using an Optical Recrystallometer (Otago Osmometers, New Zealand) as reported elsewhere.[44,45] The solutions were prepared in ultrapure MilliQ water with 9 ‰ NaCl. We measured the CPS sample (10 mg/mL = 6.6 μM), and positive and negative controls. As a positive control we used a recombinant antifreeze protein (AFP) from the sea-ice diatom *Fragilariopsis cylindrus*. The protein was provided by M. Bayer-Giraldi and produced recombinantly in *E. coli* as described previously.[44] As a negative control we used chondroitin, a capsular polysaccharide produced by an engineered *E. coli* K4.[46] All particle solutions (CPS, AFP and chondroitin) were measured at the same concentration of 6.6 μM. Furthermore, we measured a particle-free solution of MilliQ water with 9 ‰ NaCl. We injected 200 μl solution in a cold, thin glass sample tube and shock-froze the sample at −80°C. Ice was annealed in the Optical Recrystallometer for 1.5 hours at −4°C. The device was cooled by a refrigerated circulating fluid and connected to a dry air (nitrogen gas) source to avoid condensation on the sample tube surface. The intensity of the light transmitted through the sample was recorded over time, where its increase is a measure for recrystallization. The increase was reported as I_t-I_0, where I_t is the intensity at a moment t and I_0 is the initial intensity. The procedure was repeated three times for each sample.

Results

Cell growth and TEM. The presence of capsular structures around cells of *Colwellia psychrerythraea* 34H grown at 4 °C was first highlighted by classic Indian ink staining[47] (data not shown) and then confirmed by TEM analysis. TEM images (Figure 1) revealed details of the cell envelope, including the presence of a capsular structure surrounding most of the observed cells.

CPS extraction, purification and characterization. The extraction protocol used on dried *C. psychrerythraea* 34H yielded 95 mg of LOS extract. The purified sample was visualized by 14% DOC-PAGE using either silver nitrate or Alcian blue staining methods (Figure 2a, b). The silver nitrate showed the presence of only one band at low molecular masses, corresponding to LOS, which has been characterized elsewhere.[26] Instead, the Alcian blue staining method, which is sensitive to polyanionic substances, allowed us to visualize bands at higher molecular masses too. Sugar and fatty acid analysis of the sample showed the presence

mainly of galacturonic acid (GalA), glucuronic acid (GlcA), 2-amino-2-deoxy-glucose (GlcN) and 2-amino-2-deoxy-galactose (GalN), together with 3,6-dideoxyhexose, mannose and 3-hydroxylated dodecanoic acid, which belong to the LOS, confirming its presence in the aqueous extract. The molecular masses of CPS and LOS species were expected to be very different on the basis of the DOC-PAGE analysis. Nevertheless, the well-known ability of the LOS to form micellar aggregates in aqueous solution did not allow the separation of the two molecular species by size exclusion chromatography. As an alternative, the sample was hydrolyzed under mild acidic conditions to cleave the glycosidic linkage between the lipid A and the saccharidic region of the LOS. After centrifugation, the supernatant containing the CPS and the core oligosaccharidic portion of the LOS was separated from a precipitate constituted by the lipid A. The supernatant mixture was separated on a Biogel P-10 chromatography column, using pyridinium acetate buffer as eluent. Two fractions were obtained: the first one, eluted in the void volume, contained the higher molecular mass material; the second one (OS) contained species with lower molecular mass, corresponding to the core oligosaccharide of the LOS. A further purification of the higher molecular mass material on a Sephacryl S-400HR chromatography column, using ammonium hydrogen carbonate as eluent, resulted in obtaining a major fraction containing the capsular polysaccharide under study (CPS). The evaluation of the molecular mass of CPS was obtained through the static light scattering technique. The analysis indicated an average molecular weight of 1500 KDa, and allowed revealing the presence of a single distribution around 100 nm (Figure S1). The large size of the scattering object suggests that probably the CPS self-assemble in a single aggregate.

To determine monosaccharide composition a methanolysis reaction followed by an acetylation was performed on the CPS, and the obtained acetylated methyl glycosides were injected into the GC-MS. This analysis revealed the presence of GalA, GlcA, GlcN and GalN, besides a signal attributed to a threonine residue on the basis of the comparison with an authentic standard. The absence of fatty acids in the GC-MS chromatogram indicated that the LOS was definitively removed. A D configuration was identified for all the monosaccharides, whereas L was found for threonine. Finally, the methylation analysis revealed the presence of 4-substituted GlcA, 3-substituted GlcN and 3-substituted GalN. No indications about the GalA substitution were found.

CPS polysaccharide was then analyzed by mono- and two-dimensional NMR (DQF-COSY, TOCSY, ROESY, NOESY, ^{1}H-^{13}C DEPT-HSQC, ^{1}H-^{13}C HMBC, 2D *F2*-coupled HSQC). The 2D-NMR analyses allowed the complete characterization of all of the spin systems. The anomeric configurations have been deduced from the $^{1}J_{C1,H1}$ coupling constants and, *inter alia*, by $^{3}J_{H1,H2}$ and chemical shifts values.

The ^{1}H-^{13}C DEPT-HSQC NMR spectrum (Figure 3, Table 1) displayed the presence of four anomeric cross-peaks at δ 5.31/98.3 (A), 4.50/104.7 (B), 4.35/104.5 (C), and 4.36/102.3 ppm (D). The correlations present in the COSY, TOCSY and HMBC spectrum (Table 1 and Figures S2-S4) indicated a *gluco*-configuration to residues B and C and a *galacto*-configuration to residues A and D. In particular, for residue B, starting from H1 signal in the COSY and TOCSY experiments, H2 up to H5 signals were rapidly identified, due to large $^{3}J_{H,H}$ ring coupling constants. Then, the identification of H6 protons was obtained from HMBC spectrum, based on the correlations between C4 carbon atom at δ 69.8 ppm and the two H6 protons at δ 3.78/3.61 ppm. As for residue C, we observed a coincidence of the chemical shift value of its proton anomeric signal with that of D. Therefore, after identification of H2 of C at δ 3.23 ppm in the COSY spectrum, the glucuronic acid was recognized, due to the cross-peaks from this proton up to H5 in the TOCSY experiment. This last was in turn connected in the HMBC spectrum with a carboxyl signal at δ 175.4 ppm. The correlations in the TOCSY experiment of H2 of D with only H3 and H4 indicated an interruption of magnetization transfer between H4 and H5, due to the small $^{3}J_{H4,H5}$ coupling constant value, according to a *galacto*-configuration. The H5 was therefore identified in the NOESY and ROESY spectra (Figure S5 and S6) by NOE contacts between H5 and H1/H3. The galacturonic acid residue A was recognized on the basis of the presence of cross-peaks from H1 up to H4 in the TOCSY spectrum. Then, in the same experiment, starting from H4 at δ 4.09 ppm the H5 resonance was easily identified at δ 4.16 ppm.

An additional spin system of a threonine residue was present. In fact, three resonances at 1.05/20.5, 4.18/69.8 and 4.15/60.8 ppm, attributed to CH_3, CHOH and CHNH groups respectively were found. Finally, threonine carboxyl group (δ 177.2 ppm) was revealed by the long-range scalar coupling present in the HMBC experiment (Table 1, Figure S4). An integration of all anomeric signals in the ^{1}H-NMR spectrum showed a ratio of 1:1:2 (Figure S6), thus indicating a tetrasaccharide repeating unit. The stoichiometric substitution of threonine was deduced from the integration of its methyl signal at δ 1.05 ppm with that of H2 of C at δ 3.23 ppm, as indicated from the ratio of 3:1 (Figure S7).

Residue A was assigned to a 2-substituted galactopyranuronic acid as its C2 resonance was shifted downfield (δ 79.2 ppm) with respect to that of an unsubstituted galacturonic acid unit,[48] and its α configuration was deduced from the $^{1}J_{C1,H1}$ coupling constant value (181 Hz). Moreover its H5 proton showed a long range scalar connectivity with its C6 carbon atom at 171.5 ppm. This last value was shifted up-field with respect to the reference value,[48] thus indicating that the carboxyl group is involved in an amide linkage.[49] This fact indicated that threonine substitutes the position C6 of residue A, according to NOESY spectrum in H_2O/D_2O (see below). Residue C was assigned to a 4-substituted glucuronic acid, as its C4 resonance was shifted downfield (δ 81.0 ppm) with respect to the reference value,[50] and its β configuration was inferred from the $^{1}J_{C1,H1}$ (169 Hz). In addition, both its H4 and H5 protons showed a correlation in the HMBC spectrum with a carboxyl signal at δ 175.4 ppm (Figure S4).

Residue B and D were identified as a 3-substituted β-glucosamine and β-galactosamine, respectively, on the basis of $^{1}J_{C1,H1}$ values (169 Hz for both) and the correlations of their H2 protons at δ 3.75 and δ 3.84 ppm, with the nitrogen-bearing carbons at δ 56.0 and 52.0 ppm, respectively. Moreover, both residues showed downfield chemical shifts for their C3 carbons (δ 83.3 and 79.3 ppm, respectively). Both H2 protons were also shifted downfield indicating the presence of acyl substituents on the amino groups, which are acetyl groups. In fact, both methyl signals at δ 1.86 and 1.77 ppm displayed in the HMBC experiment long-range scalar couplings with signals at δ 56.0/176.4 and 52.0/176.0 ppm, respectively (Figure S4).

The sequence of residues and the confirmation of the attachment points of glycosidic linkages were obtained by an in depth analysis of the HMBC, NOESY and ROESY spectra (Figures S4-S6). Long range scalar correlations were observed in the HMBC spectrum for C1 of D (C1D) and H4 of C (H4C), H1C and C3B and H1B and C2A. The substitution of residue D by the residue A was deduced from the ROESY and NOESY experiments, as both spectra showed inter-residue dipolar couplings between H1A and H3D and H4D. Inter-residue dipolar couplings were also observed between H1D and H4C, H1C and H3B and H1B and H2A.

Finally, the amide linkage between threonine and C6 of galacturonic acid was confirmed by a NOE contact between the

amino acid NH (δ 7.60 ppm), identified in the TOCSY experiment (Figure S8), and H5 of residue A (δ 4.16 ppm), measured in a NOESY experiment in H_2O/D_2O (Figure S9).
All the above data allowed us to attribute a linear structure to the repeating unit of the capsular polysaccharide from *C. psychrerythraea* 34H, as illustrated in Figure 4.
Three-dimensional structure characterization. In order to determine the three-dimensional structure of the capsular polysaccharide, an in-depth analysis of all NMR experiments was performed. The large proton-proton coupling constants observed in residues B and C suggested that all the protons are in axial positions. Then, the large coupling between H2 and H3 in residues A and D also suggested a trans-diaxial arrangement of these hydrogens. These data, along with NOE connectivities in the NOESY spectra between 1,3-diaxial protons, unambiguously indicated that all four sugar moieties assume the classical $^4C_1$ chair conformation. Therefore, dihedral angle constraints were used to keep the sugar in this conformation during structure calculations. NOESY spectra also showed NOEs between H2A and H1B, and between H1A/H1B-H5B-H3D-H4D, H3B/H1C, H4B/H1C-H2C and H5B/H1C indicating the relative spatial orientation of the sugars. Interestingly, NOEs between H1B/H4D and H4B/H1D clearly indicated that the sugar moieties B and D were spatially close to each other. In order to build a three-dimensional model taking into account all of the experimental data, restrained molecular mechanic and dynamic calculations were performed. Considering that the molecular weight of the polysaccharide is approximately 1500 kDa, and that performing reliable structure calculations at atomic level on a such high molecular mass structure is not possible (especially considering the lack of long-range distance restraints), we opted to create a simplified model (**M1,** Figure 5a), taking into account about five repetitions of the tetramer A-B-C-D. Using the approach described in Methods, a total of 200 structures were generated. The calculations provided a mixture of isoenergetic conformers characterized by no NOE violations > 0.4 Å (Table S3).
However, the central repeat, having a more realistic environment, could be clustered in a well-defined family having a good superimposition with root mean squared difference (RMSD) values of 0.77 Å calculated on all heavy atoms of the sugar rings (Figure 7, Figure S10). Thus, the representative structure (i.e. the closest to the centroid of the cluster) of this cluster was subjected to molecular dynamics (MD) simulations to probe its thermodynamic stability and to further refine this model in explicit solvent.

Ice recrystallization inhibition assay. In order to determine if CPS actively interacts with ice, we tested its effect as ice recrystallization inhibitor. Ice grains recrystallize over time, as large crystals develop at the expense of smaller ones. Some molecules able to attach to ice, for example AFPs, inhibit recrystallization.[44,51] Due to light refraction at ice grain boundaries, light transmittance through ice is directly proportional to the size of crystals in the sample. Large ice crystals result in high light transmittance, while small crystals result in low transmittance. Therefore, the recrystallization of ice crystals can be followed recording the change of light intensity over the time. Chondroitin, an anionic polysaccharide constituted by alternating *N*-acetyl galactosamine and glucuronic acid residues, was used as negative control due to the similarity of its structure with that of CPS.
The ice recrystallization assay (Figure 6) showed that the presence of CPS inhibits recrystallization. Indeed, the light intensity change of the CPS-sample was smaller than the increase recorded for both negative controls. The chondroitin had no statistically relevant effect on ice recrystallization.

Discussion

Cold-adapted bacteria colonize a large portion of Earth's biosphere. They survive and thrive in alpine, polar and other cold regions via numerous molecular adaptations.[4] Many of the adaptive mechanisms have been deduced from genomic and proteomic data, but extracellular strategies that may contribute to surviving in extreme environments are less well investigated by such approaches. The extracellular exudates, composed primarily of exopolysaccharides, that are produced by psychrophilic and ice-dwelling microorganisms have reached a prominent position among the cryoprotectants.[14-18,21] The term exopolysaccharide includes either cell-membrane associated or totally cell-free macromolecules. When the exopolysaccharide is firmly associated with the bacterial cell surface, the microorganism presents a capsule that can be recognized by either light or electron microscopy.[52] The aim of this study was to characterize the primary and the three-dimensional structures of the capsular material produced by the stenopsychrophilic bacterium *Colwellia psychrerythraea* 34H. Furthermore, we tested whether CPS interacts with ice by assessing its ice-recrystallization inhibition activity.
C. psychrerythraea 34H has been considered a model for the study of bacterial growth and survival strategies in cold marine environments.[22] The synthesis of extracellular polysaccharides appears to be important to cold-adaptation of this strain, especially in subfreezing environments.[12,17,23,24] Data reported here unravel the structure of a capsular polysaccharide surrounding individual cells of *C. psychrerythraea* 34H (Figure 1), which in turn defines the organism's interface with its environment.
The results of chemical and spectroscopic analyses of the purified capsular material revealed a structure new among bacterial polysaccharides: a linear tetrasaccharide repeating unit containing two amino sugars and two uronic acids, of which one is amidated by a threonine (Figure 4).
Even though the glycosyl composition may be comparable to that of EPS produced by many marine bacteria, the presence of amino acids is quite uncommon.[50,53,54] Sulphates or organic acids have generally been found as substituents on the sugar backbone;[55] protein has been detected in some bacterial EPS but their relation with the sugar backbone is unknown.[56,57]
The decoration of the polysaccharide with Thr is particularly intriguing to consider. In fact, amino acid motifs are common, and crucial for the interaction with ice, in several different kinds of antifreeze proteins (AFPs).[55-57] For example, antifreeze glycoproteins (AFGPs) isolated from fish blood plasma consist of a regular tripeptide sequence of Ala-Ala-Thr with a disaccharide fragment (β-D-galactosyl-(1-3)-α-D-galactosamine) linked to the threonine residue.[58-61]
It is noteworthy that the polysaccharide described here displays a structural feature very close to that present in AFGPs. Actually, a β-*N*-acetyl-galactosamine is substituted by an α-galacturonosyl residue bearing an amide-linked threonine.
Antifreeze proteins are known to control ice growth by attaching to ice crystals by their ice-binding-site. The spacing between relevant amino acids on the ice-binding sites often resembles the atomic distances typical for the ice lattice. Several times, the amino acids show a repetitive pattern or periodic folding, thus showing regularly spaced OH groups.[62-65] The periodic folding of this kind of structures is of a particular interest, and the composition of the polysaccharide, that is composed by repetitive tetrasaccharide units. In order to determine a possible spatial arrangement of the capsular polysaccharide, all the NMR experiments were analyzed and molecular mechanic and dynamic calcu-

lations were performed. We focused our attention on a simplified model (**M1**) of the capsule comprising basically five repeats of the tetrasaccharide base unit. A number of isoenergetic conformations were obtained; only information about the local conformation adopted by the polysaccharide could be retrieved. Interesting structural features characterized the obtained models. First of all, the chains of the sugars A-B-C-D were fairly linear. Furthermore, the orientation of sugars B and D, linked to equatorial position O2 and axial position O1 of sugar A, conferred a "hairpin-like" disposition to the chains. This portion of the polysaccharide seems to be repeated in the space forming an overall "zigzag" structure, where threonines of sugars A are placed at the very corner of the polysaccharide. The analysis of the 20 ns molecular dynamics (MD) trajectories gave an idea of the flexibility of the computed structure. In particular, plotting of the angle formed by the C2 atoms of each A sugar residues (Figure 5a) allowed monitoring the hinge motions experienced by **M1** during the dynamic calculations. The angles ranged roughly from 80° to 110° and the angle formed by the residues A4-A5-A6 turned out to be the most flexible one (92.83°±17.36, Figure 5e). This result was expected considering that this angle is formed by the terminal repetitions of the molecule. Furthermore, the flexibility of the model was also monitored by plotting of three pseudo-dihedral angles formed by the C2 sugar atoms of the A residues: A1-A2-A3-A4, A2-A3-A4-A5 and A3-A4-A5-A6 (Figure 8). As depicted in Figure 8a,b, the A1-A2-A3-A4 and A2-A3-A4-A5 pseudo-dihedral angles range from a minimum of ≈20° to a maximum of ≈180°. Nevertheless, calculating the averages and the standard deviations for the aforementioned angles makes clear that the most frequent variation from the average is ±20° (see the bottom plots of Figure 8a and 8b). On the other hand, plotting the A3-A4-A5-A6 pseudo-dihedral angle values demonstrated that after about 13 ns of dynamic the terminal repetition (formed by A6-D5-C5-B5-A5 residues) rotates from the remaining part of the polysaccharide of about 320°. In this case, calculation of the standard deviation (see the bottom plots of Figure 8c) suggests that this terminal end of the polysaccharide is indeed very flexible. Altogether these data suggest that the computed model, although maintaining an overall "zigzag" arrangement, is very flexible and that the overall structure can be imagined like a spatial repetition of an hairpin-like substructure, where the threonines are placed externally and available to interact with the ice.

These results, the resemblance of our CPS structure to that of AFGPs, and the lack of sequence coding for a known AFP in the genome of *C. psychrerythraea* 34H[65] prompted us to assay for ice recrystallization inhibition activity of the *Colwellia* capsular polysaccharide purified extract. Our analyses of ice recrystallization activity suggest that CPS interacts with ice in a way resembling AFPs, further supporting structural CPS observations. Results showed that CPS has an effect on recrystallization, whereas other particles like chondroitin in our negative particle control have no statistically relevant effect. It is therefore conceivable that CPS binds to ice, pinning and immobilizing ice grain boundaries with a similar effect as that reported for AFPs. The results showed an effect less marked with respect to that displayed by a recombinant AFP from the sea-ice diatom, which is a strong inhibitor of recrystallization compared to other AFPs.[44] However, the comparison between two very different molecules, such as a polysaccharide and a protein, may not be appropriate or rigorous. Besides ice-binding patterns, the size, composition and conformation of the molecules also play a role in modulating the effect on ice. Furthermore, it should be considered that the natural concentrations of both CPS and AFP, and therefore the effective magnitude of ice activity under relevant environmental or physiological conditions remains unknown.

The only other example of a polysaccharide reported to have properties resembling AFP activity was extracted from a freeze-tolerant beetle, *Upis ceramboides*.[66] The fact that the polysaccharide examined also contained lipid leaves unresolved whether the polysaccharide or the lipid component was responsible for the activity.[66]

This study has demonstrated for the first time the existence of a capsular polysaccharide that in its purified form is endowed with ice recrystallization inhibition activity. Its unique structure, in contrast to that isolated from the beetle *U. ceramboides,* is strongly related to that of AFGPs, both for the presence of a Thr residue and for the Gal-Gal disaccharide motif.

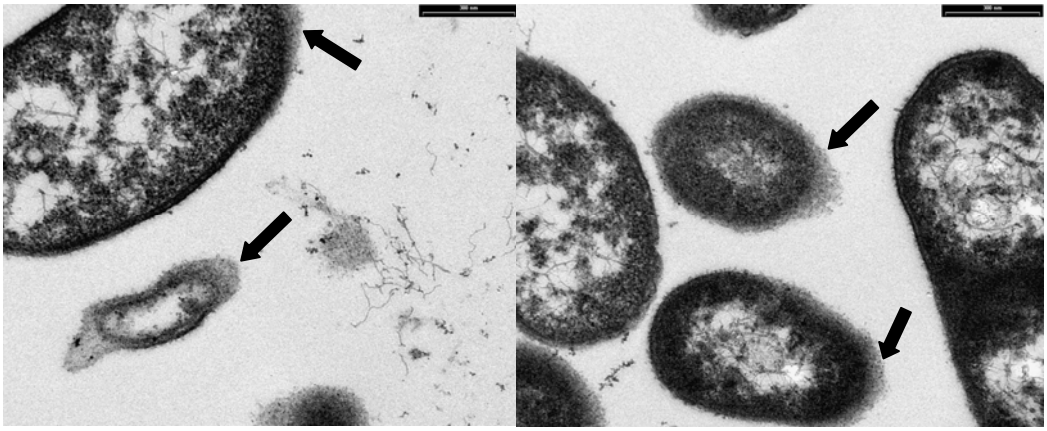

Figure 1. Transmission electron microscopy (TEM) images of thin sections of *Colwellia psychrerythraea* 34H. The black arrows indicate the bacterial capsule.

Figure 2. Analysis of the CPS fraction from *C. psychrerythraea* 34H by 14% DOC-PAGE. The gel was stained with silver nitrate (a) and Alcian blue dye (b).

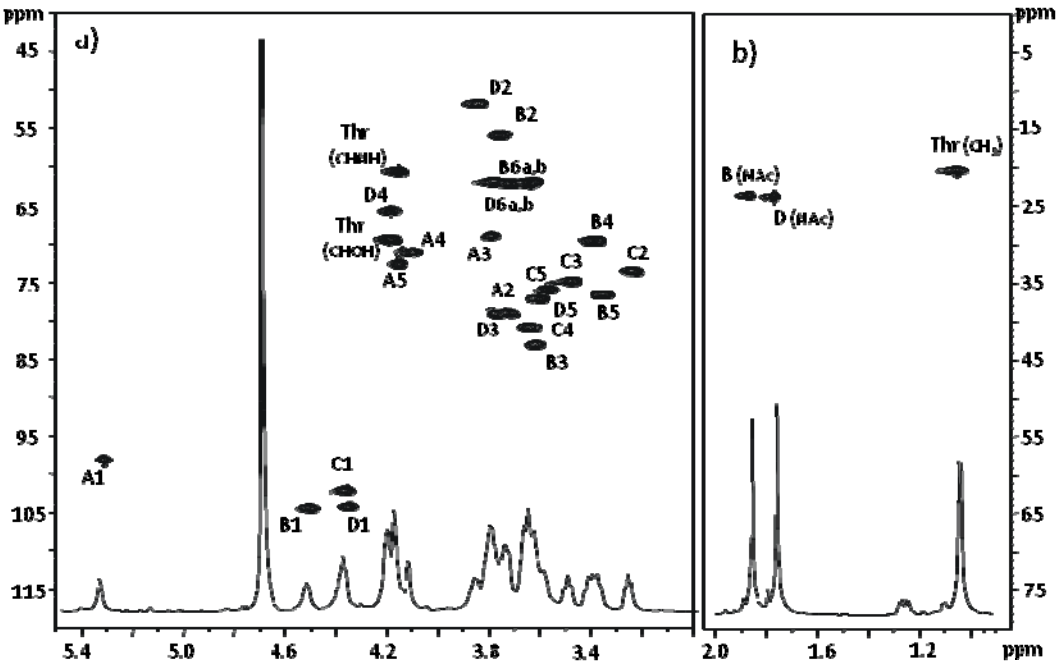

Figure 3. Carbinolic anomeric (a) and aliphatic (b) regions of $^{1}H,^{13}C$ DEPT-HSQC spectrum of CPS from *C. psychrerythraea* 34H. The spectrum was recorded in D_2O at 298 K at 600 MHz. The letters refer to residues as described in Table 1.

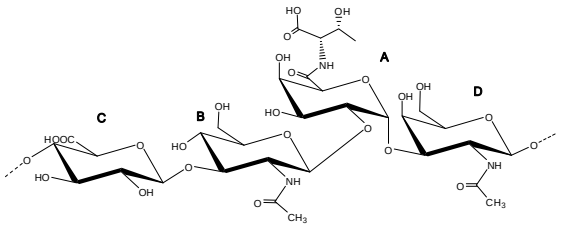

Figure 4. Primary repeating tetrasaccharide structure of the capsular polysaccharide isolated from *C. psychrerythraea* 34H.

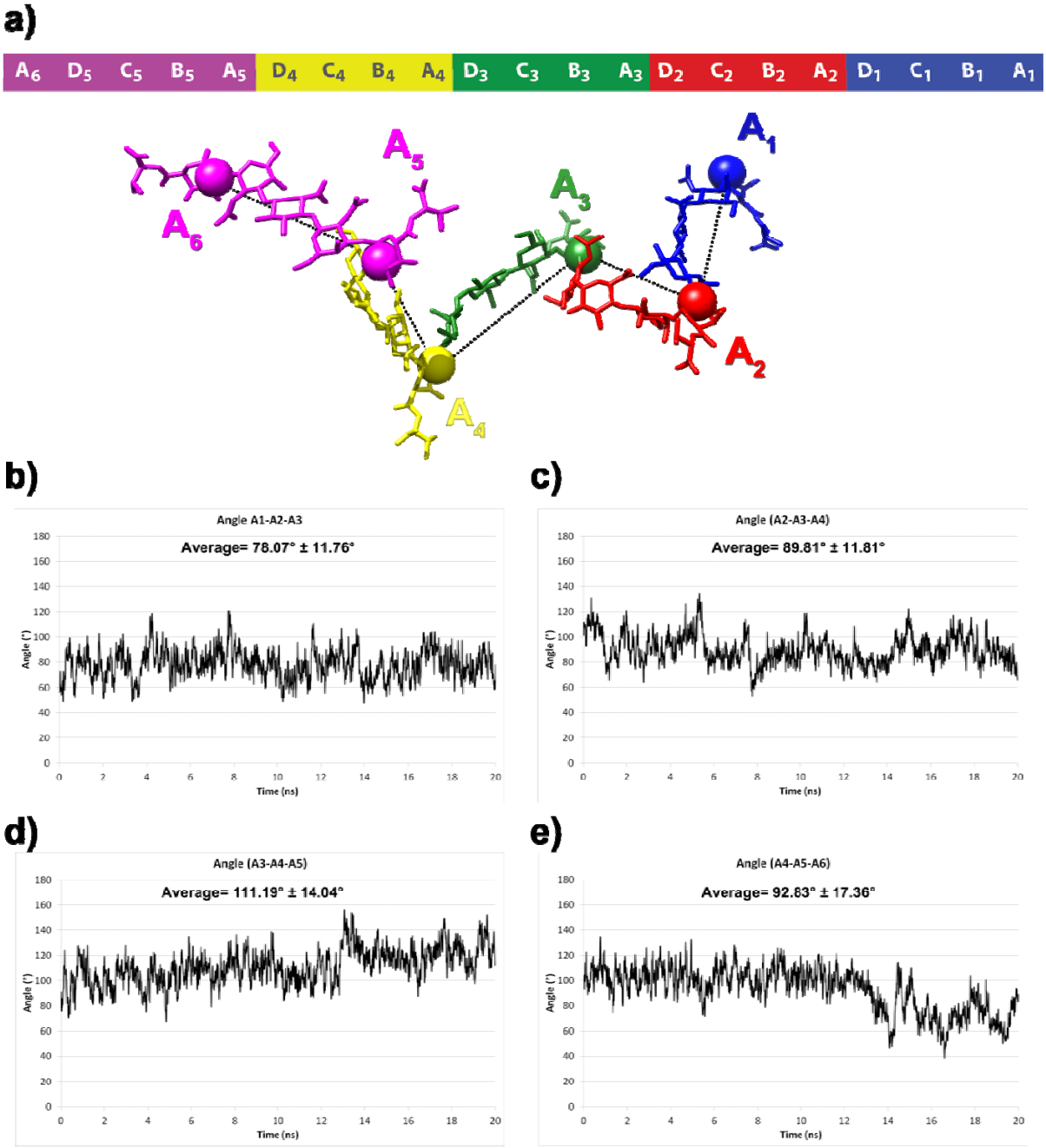

Figure 5. (a) Front view of the average **M1** structure deriving from the 20 ns MD production run together with a pictorial representation of its sugar residue sequence. Repetition 1, 2, 3 4 and 5 are represented as blue, red, green, yellow and magenta sticks, respectively. The C2 atoms of the A1-6 sugar residues, used to calculate the hinge angles are represented as spheres. Plots of the hinge angle values (°) formed by the C2 atoms of the A1-A2-A3, A2-A3-A4, A3-A4-A5 and A4-A5-A6 are represented in (b), (c), (d) and (e) insets, respectively. The degree of flexibility for each hinge angle is calculated as the standard deviation from the values obtained from the last 20 ns of simulation.

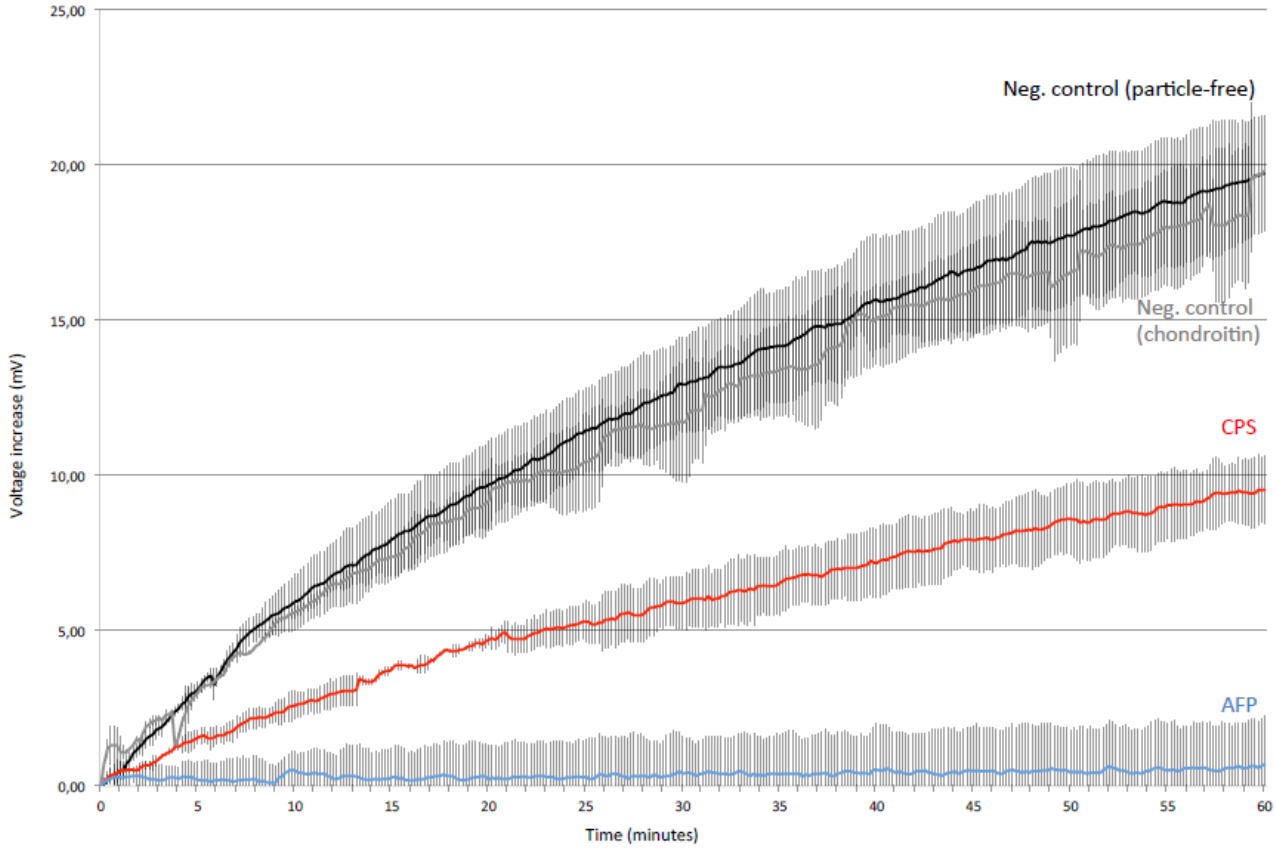

Figure 6. Recrystallization of frozen samples as assayed in the Optical Recrystallometer. The light intensity increases as a function of time is indicative for recrystallization processes of ice crystals. Measurements were performed for 1 hour at ~4°C. We measured a solution with CPS (red), a positive control with AFP from *F. cylindrus* (blue), a negative control with chondroitin (grey) and a particle-free positive control (black). The solutions were prepared in ultrapure MilliQ water with 9 ‰ NaCl, particle concentration was adjusted to 6.6 µM. The curves are an average of three samples, error bars show standard deviation.

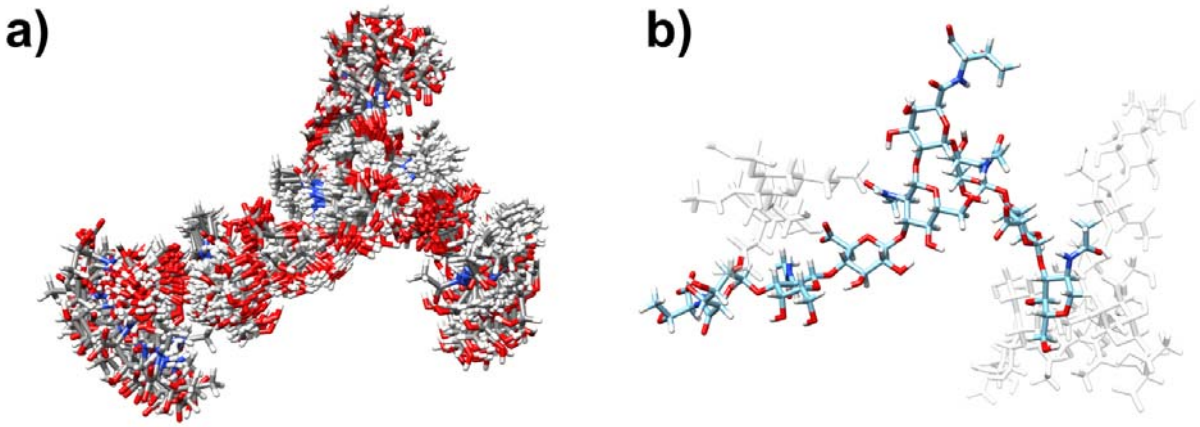

Figure 7. (a) Superimposition of the 51 conformations of **M1** belonging to the most populated cluster as calculated through annealing simulations. For clarity reasons, only the central 2 repetitions of the tetramer A-B-C-D, on which the clustering was attained, are represented. (b) Representative **M1** conformation of the most populated cluster. The central 2 repetitions of the tetramer A-B-C-D are represented as cyan sticks while the remaining repetitions are displayed as transparent white sticks.

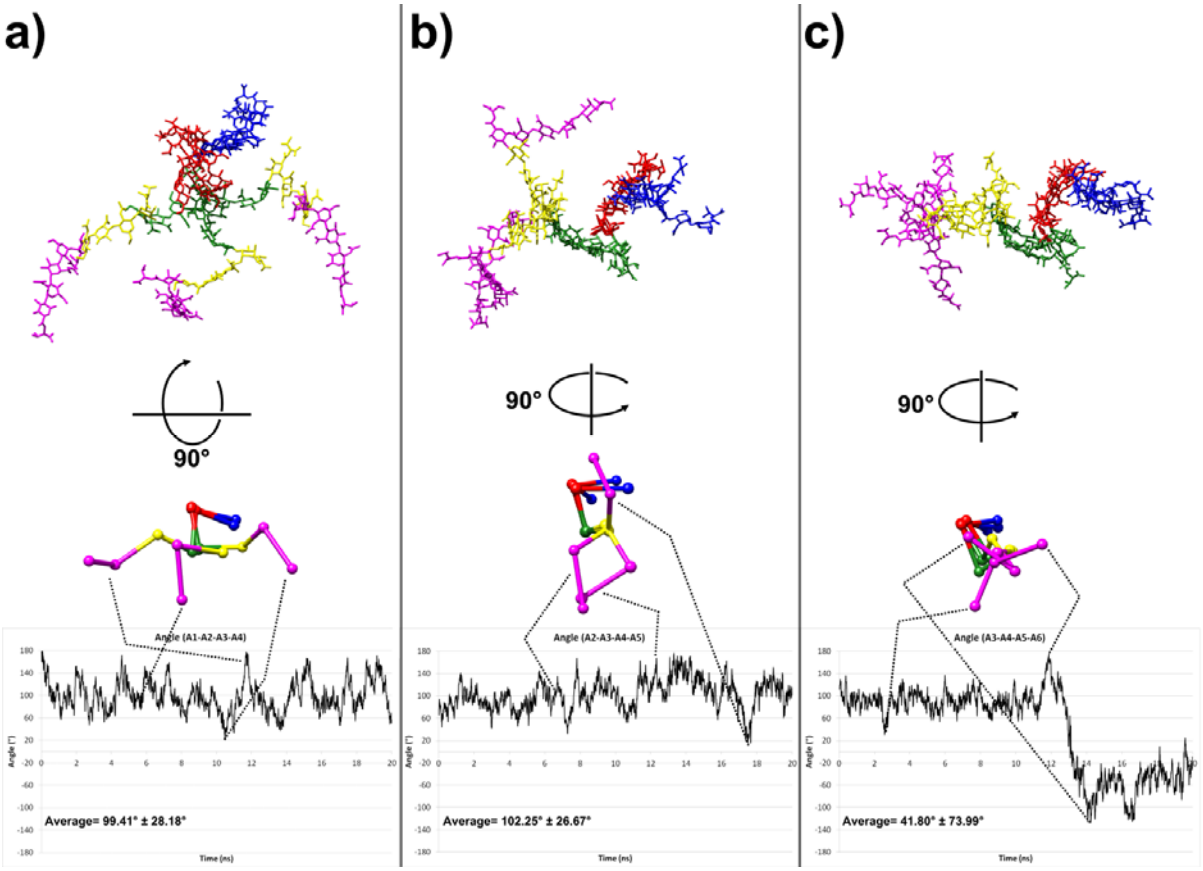

Figure 8. Three representative conformations of **M1** describing the pseudo-dihedral angles during the last 20 ns of the MD simulation formed by the C2 sugar atoms of the A residues, A1-A2-A3-A4, A2-A3-A4-A5 and A3-A4-A5-A6 depicted in a), b), and c) insets, respectively. The top of the picture depicts the three superimposed conformations describing the lowest, average and highest values of the three pseudo-dihedral angles. These are also depicted as pictorial representations (stick and balls) in the middle of the picture in a 90° rotated view to better show the changes in the dihedral angles. In the bottom of the picture the plots describing the three pseudo-dihedral angles during the 20 ns simulation are reported.

Table 1. ^{1}H and ^{13}C NMR assignments of CPS. Spectra were recorded in D_2O at 298 K. Signals at δ 5.31/98.3 ppm, previously assigned respect to acetone as internal standard (δ H 2.225 ppm and δ C 31.45 ppm), were used as reference.

Residue	H1 C1	H2 C2	H3 C3	H4 C4	H5 C5	H6a,b C6
A **2-α-D-GalpA6LThr**	5.31 98.3	3.72 79.2	3.79 69.2	4.09 71.2	4.16 72.9	- 171.5
B **3-β-D-Glc*p*NAc**	4.50 104.7	3.75 56.0	3.62 83.3	3.38 69.8	3.35 76.8	3.78-3.61 62.1
C **4-β-D-Glc*p*A**	4.35 104.5	3.23 73.9	3.48 74.9	3.65 81.0	3.59 77.3	- 175.4
D **3-β-D-Gal*p*NAc**	4.36 102.3	3.84 52.0	3.76 79.3	4.19 66.1	3.56 76.1	3.71-3.64 62.3

Additional chemical shifts:
NAc at δ 1.86/23.7 ppm (CH_3), 176.4 ppm (CO); δ 1.77/23.8 ppm (CH_3), 176.0 ppm (CO)
Thr at δ 1.05/20.5 ppm (CH_3), 4.18/69.8 ppm (CHOH), 4.15/60.8 ppm (CHNH), 177.2 ppm (COOH)

AUTHOR INFORMATION

Corresponding Authors

M. Michela Corsaro, Department of Chemical Sciences, University of Naples "Federico II", Complesso Universitario di Monte Sant'Angelo, via Cintia 4, 80126 Naples, Italy. Tel.: (+39)081-674149; Fax: (+39)081-674393; E-mail: corsaro@unina.it

M. Luisa Tutino, Department of Chemical Sciences, University of Naples "Federico II", Complesso Universitario di Monte Sant'Angelo, via Cintia 4, 80126 Naples, Italy. Tel.: (+39)081-674317; Fax: (+39)081-674393; E-mail: tutino@unina.it

Author Contributions

^These authors contributed equally.

Notes

The authors declare no competing financial interests.

ACKNOWLEDGMENT

Dedicated to the memory of Professor Alessandro Ballio (1921-2014).

We thank Prof. Luigi Paduano of Chemical Sciences Department, University of Naples "Federico II" for molecular mass determination and Prof. Alba Silipo for the valuable discussion about NMR spectra. The authors thank the Centro Interdipartimentale Metodologie Chimico Fisiche, University of Naples "Federico II" and BioTekNet for the use of the 600 MHz NMR spectrometer. This work was supported by Programma Nazionale di Ricerca in Antartide 2010 (grant PNRA 2010/A1.05), and 2013 (grant PNRA 2013/B1.03), and the Walters Endowed Professorship (to J.W.D.).

REFERENCES

(1) Cavicchioli, R. *Nat. Rev. Microbiol.* **2006**, *4*, 331-43

(2) Cavicchioli, R.; Siddiqui, K. S.; Andrews, D.; Sowers, K. R. *Curr. Opin. Biotech.***2002**, *13*, 253-261.

(3) D'Amico, S.; Collins, T.; Marx, J. C.; Feller, G.; Gerday, C. *EMBO Rep.* **2006**, *7*, 385-389.

(4) Casanueva, A., Tuffin, M., Cary, C., Cowan, D.A. *Trends Microbiol.* **2010**, *18*, 374-381.

(5) Chattopadhyay, M. K.. *J. Biosci.* **2006**, *31*, 157-165.

(6) Ummarino, S.; Corsaro, M. M.; Lanzetta, R.; Parrilli, M.; Peter-Katalinić, J. *Rapid Commun. Mass Sp*. **2003**, *17*, 2226-2232.

(7) Corsaro, M. M.; Lanzetta, R.; Parrilli, E.; Parrilli, M.; Tutino, M. L;. Ummarino, S. *J. Bacteriol.*, **2004**, *186*, 29-34.

(8) Corsaro, M. M., Pieretti, G.; Lindner, B.; Lanzetta, R.; Parrilli, E.; Tutino, M. L.; Parrilli, M. *Chemistry* **2008**, *14*, 9368-76.

(9) Carillo, S.; Pieretti, G.; Parrilli, E.; Tutino, M. L.; Gemma, S.; Molteni, M.; Lanzetta, R.; Parrilli, M.; Corsaro, M. M. *Chemistry* **2011**, *17*, 7053-7060.

(10) Ray, M. K.; Kumar, G. S.; Shivaji, S. *Microbiology* **1994**, *140*, 3217-3223.

(11) Ray, M. K.; Kumar, G. S.; Shivaji, S. *J. Bacteriol.* **1994**, *176*, 4243-4249.

(12) Huston, A. L.; Methé, B. A.; Deming, J. W. *Appl. Environ. Microbiol.* **2004**, *70*, 3321-3328.

(13) Deming, J. W. Extremophiles: cold environments. In *Encyclopedia of microbiology*. Edition 3; Lederberg, J.; Schaechter, M., Eds; Elsevier, Oxford, 2009.

(14) Krembs, C.; Deming, J. W.; Junge, K.; Eicken, H. *Deep Sea Res. Part I. Oceanogr. Res. Pap.* **2002**, *49*, 2163-2181.

(15) Krembs, C.; Deming, J. W. The role of exopolymers in microbial adaptation to sea ice In *Psychrophiles: from biodiversity to biotechnology.* Margesin, R.; Schinner, F.; Marx, J-C,; Gerday, C., Eds.; Springer-Verlag: Berlin, 2008; pp 247-264.

(16) Guézennec, J. *J. Ind. Microbiol. Biot.*. **2002**, *29*, 204-208.

(17) Krembs, C;, Eicken, H.; Deming, J. W. *US Proc. Natl. Acad. Sci.* **2011**, *108*, 3653–3658.

(18) Ewert, M.; Deming, J. W. *Biology* **2013***, 2*, 603–628.

(19) Nichols, C. M.; Lardière, S. G.; Bowman, J. P.; Nichols, P. D.; Gibson, J. A. E.; Guézennec, J. *Microb. Ecol.* **2005**, *49*, 578-589.

(20) Baker, M. G.; Lalonde, S. V.; Konhauser, K. O.; Foght, J. M. *Appl. Environ. Microbiol.* **2010**, *76*, 102-109.

(21) Sheng-Bo, L.; Xiu-Lan, C.; Hai-Lun, H.; Xi-Ying, Z.; Bin-Bin, X.; Yong, Y.; Bo, C.; Bai-Cheng, Z.; Yu-Zhong, Z. *Appl. Environ. Microbiol*. **2013**, *79*, 224.

(22) Methé, B. A.; Nelson, K. E.; Deming, J. W.; Momen, B.;Melamud, E.; Zhang, X.; Moult, J.; Madupu, R.; Nelson, W. C.; Dodson, R. J.; Brinkac, L. M.; Daugherty, S. C.; Durkin, A. S.; DeBoy, R. T.; Kolonay, J. F.; Sullivan, S. A.; Zhou, L.; Davidsen, T. M.; Wu, M.; Huston, A. L.; Lewis, M.; Weaver, B.; Weidman, J. F.; Khouri, H.; Utterback, T. R.; Feldblyum, T. V.; Fraser, C. M. *Proc. Natl. Acad. Sci. U.S.A.* **2005**, *102*, 10913-10918.

(23) Marx, J. G.; Carpenter, S. D.; Deming, J. W. *Can. J. Microbiol.* **2009**, *55*, 63-72.

(24) Ewert, M.; Deming, J. W. *Ann. Glaciol.* **2011**, *52*, 111–117.

(25) Basile, A.; Cafiero, G.; Spagnuolo, V.; Castaldo Cobianchi, R. *J. Bryol.***1994**, *18*, 69-81.

(26) Carillo, S.; Pieretti, G.; Lindner, B.; Parrilli, E.; Sannino, F.; Tutino, M. L.; Lanzetta, R.; Parrilli, M.; Corsaro, M. M. *Eur. J. Org. Chem*. **2013**, 3771-3779.

(27) Galanos, C.; Lüderitz, O.; Westphal, O. *Eur. J. Biochem*. **1969**, *9*, 245-249.

(28) Westphal, O.; Jann, K. *Methods Carbohydr. Chem*. **1965**, *5*, 83-91.

(29) Laemmli, U. K. *Nature* **1970**, *227*, 680-685.

(30) Tsai, C. M.; and Frasch, C. E. *Anal. Biochem.* **1982**, *119*, 115-119

(31) Al-Hakim, A.; Linhardt, R. J. *Electrophoresis* **1990**, *11*, 23-28

(32) Simeone, L.; Mangiapia, G.; Vitiello, G.; Irace, C.; Colonna, A.; Ortona, O.; Montesarchio, D.; Paduano, L. *Bioconjugate Chem.* **2012**, *23*, 758-770.

(33) Ciucanu, I.; Kerek, F. *Carbohydr. Res*. **1984**, *131*, 209-217.

(34) Forsberg, L. S.; Ramadas Bhat, U.; Carlson, R. W. *J. Biol. Chem*. **2000**, *275*, 18851-18863.

(35) Leontein, K.; Lindberg, B.; Lönngren, J. *Carbohydr. Res*. **1978**, *62*, 359-362.

(36) Woods Group. (2005-2014) GLYCAM Web. Complex Carbohydrate Research Center, University of Georgia, Athens, GA. (http://www.glycam.com)

(37) Case, D.A.; Babin, V.; Berryman, J.T.; Betz, R.M.; Cai, Q.; Cerutti, D.S.; Cheatham, T.E. III; Darden, T.A.; Duke, R.E.; Gohlke, H.; Goetz, A.W.; Gusarov, S.; Homeyer, N.; Janowski, P.; Kaus, J.; Kolossváry, I.;

Kovalenko, A.; Lee, T.S.; LeGrand, S.; Luchko, T.; Luo, R.; Madej, B.; Merz, K.M.; Paesani, F.; Roe, D.R.; Roitberg, A.; Sagui, C.; Salomon-Ferrer, R.; Seabra, G.; Simmerling, C.L.; Smith, W.; Swails, J.; Walker, R.C.; Wang J.; Wolf, R.M.; Wu, X.; Kollman, P.A. AMBER 14th ed.; University of California, San Francisco, **2014.**

(38) Kirschner, K.N.; Yongye, A.B.; Tschampel, S.M.; Daniels, C.R.; Foley, B.L; Woods, R.J. *J. Comput. Chem.* **2008**, *29*, 622– 655

(39) Jorgensen, W. L.; Chandrasekhar, J.; Madura, J. D.; Impey, R. W; Klein, M. L. *J. Chem. Phys.* **1983**, *79*, 926– 935

(40) (a) Darden, T.; York, D.; Pedersen, L. *J. Chem. Phys.* **1993**, *98*, 10089– 10092 (b) Essmann, U.; Perera, L.; Berkowitz, M. L.; Darden, T.; Lee, H.; Pedersen, L. G. *J. Chem. Phys*. **1995**, *103*, 8577– 8593

(41) van Gunsteren, W. F.; Berendsen, H. J. C. *Mol. Phys.* **1977**, *34*, 1311–1327

(42) Shao, J.; Tanner, S. W; Thompson, N; Cheatham, T. E; III. *J. Chem. Theory Comput.* **2007**, *3*, 2312– 2334

(43) Pettersen, E.F.; Goddard, T.D.; Huang, C.C.; Couch, G.S.; Greenblatt, D.M.; Meng, E.C.; Ferrin, T.E. *J Comput Chem.* **2004**, *25*,1605-12

(44) Bayer-Giraldi, M.; Weikusat, I.; Besir, H.; Dieckmann, G. *Cryobiology* **2011**, *63*, 210-219

(45) Bayer-Giraldi, M.; Jin, E. S.; Wilson, P. W.; Characterization of Ice Binding Proteins from Sea Ice Algae In *Plant Cold Acclimation, Methods in Molecular Biology*, Hincha, D. K.; Zuther, E., Eds.; Springer: New York 2014; *1166*.

(46) Cimini, D.; De Rosa, M.; Carlino, E.; Ruggiero, A.; Schiraldi, C. *Microb. Cell. Fact*. **2013**, *12*, 46-57.

(47) Taylor, W. H.; Juni, E. *J. Bacteriol.* **1960**, *81*, 688.

(48) Ramos, M.L.D.; Caldeira, M.M.M.; Gil, V.M.S. *Carbohydr. Res*. **1996**, *286*, 1-15.

(49) Sidorczyk, Z.; Swierzko, A.; Knirel, Y. A.; Vinogradov, E. V.; Chernyak, A. Y.; Kononov, L. O.; Cedzynski, M.; Rozalski, A.; Kaca, W.; Shashkov, A. S.; Kochetkov, N. K. *Eur. J. Biochem*. **1995**, *230*, 713-721

(50) Bock, K.; Pedersen, C. *Adv. Carbohydr. Chem. Biochem*. **1983**, *41*, 27-66.

(51) Knight, C. A.; Duman., J. A. *Cryobiology* **1986**, *23*, 256-262

(52) Sutherland, I. W. Biotechnology of microbial exopolysaccharides. In *Cambridge Studies in Biotechnology;* Sir Baddiley, J.; Carey, N. H.; Higgins, I. J.; Potter, W. G., Eds. Cambridge University Press, Cambridge, 1990; pp 1-11.

(53) Komandrova, N. A.; Isakov, V. V.; Tomshich, S. V.; Romanenko, L. A.; Perepelov, A. V.; Shashkov, A. S. *Biochemistry (Moscow),* **2010***, 75*, 623-628.

(54) Palusiak, A. *Carbohydr. Res*. **2013**, *380*, 16-22.

(55) Nichols, C. M.; Guézennec, J.; Bowman, J. P. *Mar. Biotechnol.* **2005,** *7*, 253-271.

(56) Mancuso Nichols, C.; Lardière, S. G.; Bowman, J. P.; Nichols, P. D.; Gibson, J. A.; Guézennec, J. *Microbial ecology* **2005**, *49*, 578-589.

(57) Daley, M. E.; Sykes, B. D. *Protein Science* **2003**, *12*, 1323-1331.

(58) Ben, N. R. *Chembiochem* **2001**, *2*, 161-166

(59) Harding, M. M.; Anderberg, P. I.; Haymet, A. D. J. *Eur. J. Biochem.*, **2003**, *270*, 1381–1392.

(60) Lin, F.; Davies, P. L.; Graham, L. A. *Biochemistry* **2011**, *50*, 4467-4478.

(61) Graether, S. P.; Kuiper, M. J.; Gagné, S. M.; Walker, V. K.; Jia, Z.; Sykes, B. D.; Davies, P. L. *Nature.* **2000**, *406*, 325-328.

(62) Jia, Z.; Davies, P. L. *Trends Biochem. Sci*. **2002**, *27*, 101-110.

(63) Scotter, A.J.; Marshall, C. B.; Graham, L. A.; Gilbert, J. A.; Granham, C. P.; Davies, P. L. *Cryobiology*, **2006**, *53*, 229-239.

(64) Pertaya, N.; Marshall, C. B.; Celik, Y.; Davies, P. L.; Braslavsky, I. *Biophys. J*. **2008**, *95*, 333-341.

(65) Raymond, J. A.; Fritsen, C.; Shen, K. *FEMS Microbiol. Ecol.* **2007**, *61*, 214-221.

(66) Walters, K. R.; Serianni, A. S.; Sformo, T.; Barnes, B. M.; Duman, J. G. *Proc. Natl. Acad. Sci.* **2009**, *106*, 20210-20215.

For Table of Contents only